Subunit and small-molecule interaction of ribonucleotide reductases via surface plasmon resonance biosensor analyses

Mikael Crona[1], Ernst Furrer[1,3], Eduard Torrents[1,4], David R.Edgell[2] and Britt-Marie Sjöberg[1,5]

[1]Department of Molecular Biology and Functional Genomics, Stockholm University, SE-10691 Stockholm, Sweden, [2]Department of Biochemistry, Schulich School of Medicine and Dentistry, The University of Western Ontario, London, ON N6A 5C1, Canada, [3]Present address: Federal Office for the Environment (FOEN), Waste Management, Chemicals and Biotechnology Division, CH-3003 Berne, Switzerland and [4]Present address: Institute for Bioengineering of Catalonia (IBEC), Cellular Biotechnology, Scientific Park of Barcelona, Edifici Helix, Baldiri Reixac 15-21, ES-08028 Barcelona, Spain

[5]To whom correspondence should be addressed.
E-mail: britt-marie.sjoberg@molbio.su.se

Edited by Lars Baltzer

Ribonucleotide reductase (RNR) synthesizes deoxyribonucleotides for DNA replication and repair and is controlled by sophisticated allosteric regulation involving differential affinity of nucleotides for regulatory sites. We have developed a robust and sensitive method for coupling biotinylated RNRs to surface plasmon resonance streptavidin biosensor chips via a 30.5 Å linker. In comprehensive studies on three RNRs effector nucleotides strengthened holoenzyme interactions, whereas substrate had no effect on subunit interactions. The RNRs differed in their response to the negative allosteric effector dATP that binds to an ATP-cone domain. A tight RNR complex was formed in *Escherichia coli* class Ia RNR with a functional ATP cone. No strengthening of subunit interactions was observed in the class Ib RNR from the human pathogen *Bacillus anthracis* that lacks the ATP cone. A moderate strengthening was seen in the atypical *Aeromonas hydrophila* phage 1 class Ia RNR that has a split catalytic subunit and a non-functional ATP cone with remnant dATP-mediated regulatory features. We also successfully immobilized a functional catalytic NrdA subunit of the *E.coli* enzyme, facilitating study of nucleotide interactions. Our surface plasmon resonance methodology has the potential to provide biological insight into nucleotide-mediated regulation of any RNR, and can be used for high-throughput screening of potential RNR inhibitors.
Keywords: *Bacillus anthracis*/biotin-streptavidin immobilization/inhibitors/interaction constants/nucleotides

Introduction

Ribonucleotide reductase (RNR) catalyzes the reduction of ribonucleotides to deoxyribonucleotides. As this is the only pathway for *de novo* synthesis of DNA building blocks virtually all organisms' growth and survival are dependent on RNR providing deoxyribonucleotides for DNA synthesis and repair (Nordlund and Reichard, 2006; Mathews, 2006; Torrents *et al.*, 2008). An unbalanced production of the four deoxyribonucleotides leads to enhanced mutational rates (Mathews, 2006). RNRs circumvent this potential hazard via sophisticated allosteric regulation (Nordlund and Reichard, 2006; Torrents *et al.*, 2008) involving an allosteric specificity site that binds ATP, dATP, dTTP or dGTP. The specificity site determines what substrate will be reduced in the active site, i.e. one and the same enzyme can reduce four different substrates. Depending upon the class of RNR, the substrates will either be ADP, GDP, CDP and UDP or ATP, GTP, CTP and UTP (Torrents *et al.*, 2008). In addition to the specificity site, many RNRs also possess an N-terminal ATP cone (Aravind *et al.*, 2000) carrying a second allosteric regulatory site called the overall activity site (Nordlund and Reichard, 2006; Torrents *et al.*, 2008). The ATP cone domain binds ATP or dATP and acts as an on/off switch for enzyme activity: binding of dATP inhibits catalysis while binding of ATP to both allosteric sites does not. The overall activity site binds dATP with considerably weaker affinity compared with the specificity site.

Class I RNRs are aerobic enzymes, specific for ribonucleoside diphosphate substrates, and are found in many bacterial and bacteriophage genomes, and in almost all eukaryotic genomes. The catalytic subunits of class I enzymes are encoded by the gene *nrdA* for subclass Ia, or *nrdE* for subclass Ib. The corresponding proteins differ by the presence of an ATP cone in NrdA, whereas NrdE lacks the N-terminal ATP-cone domain. Both the NrdA and NrdE proteins contain the allosteric specificity site and the active site and are collectively referred to as the α-subunit. The enzymatically active $\alpha_2\beta_2$ holoenzyme of either NrdA or NrdE is formed in a complex with the β subunit (NrdB for class Ia, NrdF for class Ib), which harbors a radical that is propagated to the α-subunit thereby initiating catalysis. At low protein concentrations the α-component from many species is in a nucleotide-dependent monomer/dimer (α/α_2) equilibrium, whereas the β-component is a dimer (β_2) even at low protein concentrations (Rofougaran *et al.*, 2006; Rofougaran *et al.*, 2008; Crona *et al.* unpublished).

It was first shown in ultracentrifugation studies with class Ia RNR from *Escherichia coli* that nucleotides affect the interactions between NrdA and NrdB (Brown and Reichard, 1969a,b). Subsequently, class I RNR subunit interactions have been measured in enzymatic assays (Climent *et al.*, 1991), by biosensor analyses (Ingemarson and Thelander, 1996; Kasrayan *et al.*, 2004), and using gas-phase electrophoretic mobility macromolecule analysis (GEMMA) (Rofougaran *et al.*, 2006; Rofougaran *et al.*, 2008). Whereas

ultracentrifugation studies, such as gel exclusion chromatography, are not ideal when many different combinations of substrates and effectors are tested, the activity-based method only works in the presence of both effectors and substrates. Biosensor analyses require optimization of immobilization conditions for each RNR component, and have so far only proved successful for NrdB proteins. GEMMA is a high-resolution technique requiring volatile buffers and has restrictions on protein and nucleotide concentrations. All these methods, with the exception of surface plasmon resonance (SPR), are readily applicable to RNRs from any organism. In a recently published method fluorophore-labeled His-tagged *E.coli* NrdB was used to measure the interaction with *E.coli* NrdA (Hassan *et al.*, 2008), but this method requires the introduction of three site-specific mutations in the NrdB protein and is specific for *E.coli* class Ia RNR. For studies of nucleotide interactions with α-components, equilibrium dialysis and ultrafiltration techniques have been important in revealing the nucleotide-binding affinities and postulating the number of allosteric sites prior to high-resolution structures of RNRs (Brown and Reichard, 1969a,b; von Döbeln and Reichard, 1976; Nordlund *et al.*, 1990; Ormö and Sjöberg, 1990; Uhlin and Eklund, 1994; Eriksson *et al.*, 1997). However, these methods are laborious and not suitable for high-throughput screening of small-molecule RNR inhibitors, such as potential antibacterial, antiviral and anticancer compounds, and cannot detect interactions weaker than 0.2 mM. A comprehensive analysis of RNR subunit interactions in the presence and absence of nucleotides would contribute to a deeper understanding of allosteric regulatory mechanisms and stimulate the development of RNR inhibitors.

To address the interactions involving RNRs and to gain insight into its allosteric regulation we have developed a SPR-based methodology based on biotinylated RNR coupled via a 30.5 Å linker. We established the method's usefulness in a comprehensive study of subunit interactions under the influence of allosteric effectors and substrates for three different class I RNRs. The *Escherichia coli* class Ia holoenzyme with a functional ATP cone is the best-characterized RNR with known three-dimensional structures (Nordlund *et al.*, 1990; Uhlin and Eklund, 1994; Eriksson *et al.*, 1997). *Bacillus anthracis* is the causative agent of anthrax (Mock and Fouet, 2001) and has a class Ib RNR that lacks the ATP cone (Torrents *et al.*, 2005). The *Aeromonas hydrophila* phage Aeh1 class Ia RNR has a non-functional ATP cone and is unique to other class I RNRs in having a split NrdA component (Friedrich *et al.*, 2007). The N-terminal part (NrdA-a) contains the non-functional ATP cone, the specificity site and some essential active site residues, and the C-terminal part (NrdA-b) contains the other essential active site residues and a C-terminal cysteine pair involved in turnover. In contrast to a previous SPR-based study (Kasrayan *et al.*, 2004), we measured holoenzyme interaction affinities in agreement with activity assay-based affinity data in solution (Climent *et al.*, 1991; Kasrayan *et al.*, 2004). We found that effector nucleotides strengthen holoenzyme interactions in all studied RNRs, whereas substrate had no effect on the subunit interaction strengths in any of the three RNR systems. The presence of dATP strengthened the subunit interactions drastically in the *E.coli* class Ia RNR, but not in the *B. anthracis* class Ib RNR, reflecting the presence and absence of the ATP-cone domain. Interestingly, subunit interactions in the Aeh1 RNR with a non-functional ATP cone were only moderately strengthened by dATP. Finally, we show that our SPR method can be used to monitor the RNR–small molecule interactions as we could, for the first time, study nucleotide binding to a functionally preserved immobilized *E coli* NrdA.

Materials and methods

Bacterial strains, expression of RNR proteins

E.coli BL21(DE3) (Novagen) or MC1009 were used for over-expression of *E.coli* RNR proteins NrdA, NrdB and NrdB-His$_6$ (R2-His$_6$) as previously described (Sjöberg *et al.*, 1986; Larsson Birgander *et al.*, 2004; Kasrayan *et al.*, 2004; Larsson Birgander *et al.*, 2005). The Aeh1 phage NrdA-a/NrdA-b and NrdB proteins were expressed as described (Friedrich *et al.*, 2007). The *B. anthracis* NrdF protein was expressed as described (Torrents *et al.*, 2005). *Bacillus anthracis* NrdE protein was expressed in a similar manner from a cloned version of the *B. anthracis* nrdE gene in the pET28a vector (Novagen) (Torrents *et al.* to be published).

Purification of RNR proteins

Purification of *E.coli* NrdA was performed as described (Larsson Birgander *et al.*, 2005) with minor modifications. After phenyl-sepharose column purification, the NrdA protein fractions were desalted using a NAP^{TM}25 column (GE Healthcare), followed by further purification on a Q Sepharose® 16/10 HP column (GE Healthcare) with a gradient from 0 to 1 M NaCl in 50 mM Tris–HCl, pH 7.6, 2 mM dithiothreitol (DTT) buffer (buffer B). Peak NrdA fractions were pooled and concentrated using an Amicon Ultra-15 Ultracell with 50-kDa cutoff (Millipore), and resuspended in buffer B. The NrdA protein was 90–95% pure as judged by SDS-PAGE, and had a specific activity of 1560 U/mg. The NrdB protein purification was performed as previously described (Sjöberg *et al.*, 1986), and NrdB containing fractions were pooled, concentrated and washed in Amicon Ultra-15 Ultracell with a 30-kDa cutoff (Millipore). The resulting purified NrdB protein was 85–90% pure as judged by SDS-PAGE. The NrdB-His$_6$ protein was purified as described (Kasrayan *et al.*, 2004). Iron reconstitution of *E.coli* NrdB and NrdB-His$_6$ was performed as previously described (Atkin *et al.*, 1973; Torrents *et al.*, 2005) resulting in a specific activity of 3740 U/mg, 3.1–3.3 Fe per dimer and 0.9–1.0 Tyr• per dimer. The Aeh1 phage NrdA-a/NrdA-b (specific activity of 94 U/mg) and NrdB proteins, and the *B. anthracis* NrdF protein were purified as described (Torrents *et al.*, 2005; Friedrich *et al.*, 2007). Crude extracts of the *B. anthracis* NrdE protein was prepared as described (Torrents *et al.*, 2005), and purified on a Hi Load® 16/10 Phenyl Sepharose® high performance (GE Healthcare) column by applying a 0.75–0 M gradient of ammonium sulfate in buffer B. NrdE containing fractions were pooled, concentrated and washed with buffer B in Centricon tubes with 50-kDa cutoff (Millipore). The obtained NrdE protein was ≥95% pure and had a specific activity of 6.0 U/mg (Torrents *et al.*, to be published). Iron reconstitutions of Aeh1 phage NrdB (specific activity of 94 U/mg, 2.9 Fe per dimer, 0.47 Tyr• per dimer) and *B. anthracis* NrdF (specific activity of 7.1 U/mg, 3.0 Fe per dimer, 0.55 Tyr• per dimer)

were performed as previously described (Atkin *et al.*, 1973; Torrents *et al.*, 2005; Friedrich *et al.*, 2007).

Biotinylation of RNR proteins

To a 25 µM solution of *E.coli* NrdA or NrdB protein in $1\times$ phosphate-buffered saline (Sambrook *et al.*, 1989), a 1- to 100-fold molar excess of 10 mM aqueous EZ-Link® Sulfo-NHS-LC-LC-Biotin (Pierce Biotechnology Inc.) was added and incubated for 3 h at 4°C with rotation. Excess biotin linker was removed by gel filtration using a NAP™-5 column (GE Healthcare) with 50 mM HEPES, pH 7.6 as eluent. The eluate was concentrated using Amicon Microcon 30 kDa (NrdB) or 50 kDa (NrdA) cut-off filters (Millipore). A spectrophotometric determination of the biotin level was performed using the HABA/AVIDIN reagent (Sigma-Aldrich) and protein concentration by absorption with theoretical extinction coefficients $\varepsilon_{280-310}$ of 178 430 M^{-1} cm^{-1} for dimeric protein NrdA and 125 180 M^{-1} cm^{-1} for dimeric protein NrdB (http://www.expasy.org/cgi-bin/protparam). A 2-fold molar excess of biotin linker reagent was required to achieve an average of one biotin molecule per *E.coli* NrdA protein dimer while a 4-fold excess was necessary to achieve the same biotinylation level of the NrdB protein. The same protocol was used for biotinylation of the Aeh1 phage NrdB (theoretical extinction coefficient $\varepsilon_{280-310}$ of 121 825 M^{-1} cm^{-1} for dimeric NrdB), and the *B. anthracis* NrdF protein (theoretical extinction coefficient $\varepsilon_{280-310}$ of 96 720 M^{-1} cm^{-1} for dimeric NrdF). Both proteins were incubated with a 3-fold molar excess of biotin linker reagent.

Activity assays

Escherichia coli RNR activity was measured by the [3H]-CDP assay at 25°C for 10 min as described (Thelander *et al.*, 1978). In general, assays contained 33 mM HEPES, pH 7.6, 11 mM $Mg(CH_3COO)_2$, 13 µM thioredoxin, 0.5 µM thioredoxin reductase, 30 µM EDTA, 0.4 mM NADPH and 1.5 mM ATP. One subunit was held constant at a concentration of 0.06 µM, while the other subunit was applied in 10-fold molar excess; biotinylated proteins were always constant at 0.06 µM. The enzyme reaction was initiated by addition of [3H]-CDP substrate to a final concentration of 0.5 mM. A comparative assay of the enzymatic activity in standard and SPR buffer with DTT as reductive agent and 0.1 mM dTTP as effector was conducted (Table I). Both assays contained 0.1 µM NrdA, 0.3–0.8 µM NrdB, 75 mM DTT, 0.1 mM dTTP and 0.5 mM [3H]-CDP; the standard assay buffer also contained 33 mM HEPES pH 7.6, 11 mM $Mg(CH_3COO)_2$, while the SPR buffer also contained 10 mM HEPES pH 7.4, 0.15 M NaCl, 0.005% (v/v) P20 and 20 mM $MgCl_2$.

Wild-type and biotinylated phage Aeh1 NrdB proteins were assayed at 25°C for 10 min. The assay mixture contained 30 mM HEPES pH 7.5, 30 mM $Mg(CH_3COO)_2$, 30 mM DTT, 5 mM ATP, 0.7 mM [3H]-CDP, 0.22 µM NrdA and 0.12 µM NrdB/biotinylated-NrdB. For the comparative assays of Aeh1 enzyme activity under standard and SPR conditions, both buffers contained 0.11 µM NrdA, 1.9 µM NrdB, 30 mM DTT, 1 mM dTTP and 0.7 mM [3H]-CDP; the standard buffer also contained 30 mM HEPES pH 7.5 and 30 mM $Mg(CH_3COO)_2$, while the SPR buffer also contained 10 mM HEPES pH 7.4, 0.15 M NaCl, 0.005% (v/v) P20 and 10 mM $MgCl_2$. The strength of subunit interactions for the Aeh1 phage NrdA-a/NrdA-b and NrdB protein in the

Table I. Specific activities of *E.coli*, Aeh1 phage, and *B. anthracis* RNRs in standard assay buffer compared with the SPR buffer A used in this study

Type of RNR	Specific activity[a] (U/mg)	
	Standard assay buffer	SPR buffer A
E.coli class Ia	199 ± 15	267 ± 13
Aeh phage class Ia	376 ± 47	266 ± 8
B. anthracis class Ib	1.18 ± 0.02	1.33 ± 0.02

[a]Values are based on two to seven determinations of *E.coli* NrdA, Aeh1 phage NrdA, or *B. anthracis* NrdE activity in the presence of 75, 30 and 10 mM DTT, respectively, while the respective effectors were 0.1 mM dTTP, 5 mM ATP and 0.2 mM dATP, all as described in Material and Methods.

presence of 1 mM ATP was determined according to published protocols (Climent *et al.*, 1991) in the following buffer conditions: 30 mM HEPES pH 7.5, 30 mM $Mg(CH_3COO)_2$, 30 mM DTT, 1 mM ATP, 0.7 mM [3H]-CDP, 0.005 µM NrdB and 0.005–1 µM NrdA or 0.02 µM NrdB and 0.02–1 µM NrdA.

Biotinylated and unmodified *B. anthracis* NrdF were assayed at 37°C for 20 min in the following assay mixture: 50 mM Tris–HCl, pH 7.5, 10 mM DTT, 0.2 mM dATP, 20 mM $Mg(CH_3COO)_2$, 10 µM NrdE, 2.5 µM NrdF and 0.8 mM [3H]-CDP. For the comparative assay of enzymatic activity under standard and SPR conditions, each buffer was supplemented with DTT and dATP. Both assays contained 7.5 µM NrdE, $\leq$54 µM NrdF, 10 mM DTT, 1 mM dATP and 1 mM [3H]-CDP. In addition, the standard assay buffer contained 30 mM Tris–HCl, pH 7.5 and 20 mM $Mg(CH_3COO)_2$, whereas the SPR buffer contained 10 mM HEPES, pH 7.4, 0.15 M NaCl, 0.005% (v/v) P20 and 20 mM $MgCl_2$.

SPR biosensor experiments

All SPR experiments were performed on a BIAcore 3000 biosensor instrument using streptavidin sensor chips (SA sensor chips, GE Healthcare). A sterile-filtered and degassed mixture of 10 mM HEPES, pH 7.4, 0.15 mM NaCl, 10 mM $MgCl_2$, 2 mM DTT and 0.005% (v/v) P20 was used as running buffer (buffer A). Addition of 1 mM EDTA, or increasing the $MgCl_2$ concentration to 20 mM, did not affect the binding results. When required, substrates and/or effector nucleotides were included in the running buffer. All SPR biosensor experiments were carried out at 25°C using flow rates between 30 and 90 µl/min.

Escherichia coli NrdB-His6 was captured to CM5 carboxymethylated dextran sensor chips (GE Healthcare) as described (Kasrayan *et al.*, 2004). Prior to immobilization of biotinylated proteins, sensor chips were conditioned with three 1-min injections of 1 M NaCl in 50 mM NaOH after priming in buffer A without DTT. We noted that the capacity to bind ligand was reduced if the sensor chip had been exposed to DTT. Biotinylated RNR proteins (0.4–100 µM) were captured on the sensor chips at a flow rate of 2–10 µl/min. The amount of immobilized protein was 3600–5260 resonance units (RU) for *E.coli* NrdA, 1200–3700 RU for *E.coli* NrdB, 2500–4400 RU for Aeh1 phage NrdB and 200–1000 RU for *B. anthracis* NrdF. These levels gave a high specific binding to the immobilized surface relative to the non-specific binding. The RU of the biosensor are

directly proportional to mass and correspond to 1 pg/mm^2 of bound mass per RU (Jönsson *et al.*, 1991).

E.coli NrdA-NrdB interactions

At least six different NrdA concentrations were injected in random order in each experiment. The concentration range was 10 nM to 1 μM NrdA in the presence of dATP, 75 nM to 5 μM NrdA in the presence of dTTP, 75 nM to 3 μM NrdA in the presence of ATP, 10 nM to 2.5 μM NrdA in the presence of both ATP and dTTP, and 0.25 μM to 10 μM NrdA in the absence of effector. These ranges gave a binding response of 20–80% of saturated binding. Double samples without NrdA, and one sample with a single NrdA concentration, were included as controls in each experiment. Prior to injection the baseline was allowed to stabilize for 30 s, followed by a 2-min injection of analyte buffer. The binding capacity was 19–43% of the theoretical maximum, and the obtained K_D values were not affected by variations in the binding capacity. A blank flow cell deactivated with biotin was used as reference flow cell during all experiments and the non-specific binding to the reference cell varied for the studied NrdA–NrdB interactions where dATP experiments showed an non-specific binding of ≤6% while the non-specific binding in presence of substrate, dTTP, or substrate plus dTTP was generally higher (≤15%). After injection the NrdA protein was allowed to dissociate in buffer without NrdA protein for 2 min, followed by injection of 15 μl 0.5 M KCl, and 8 min dissociation in running buffer. Binding experiments involving the amino-coupled *E.coli* NrdB-His$_6$ protein were treated similarly. All experiments were repeated two to three times, and the binding capacity of the immobilized *E.coli* NrdB proteins were maintained for 2–3 days on the sensor chips.

Aeh1 phage (NrdA-a/NrdA-b)−NrdB interactions

Experiments with the phage Aeh1 NrdA-a/NrdA-b proteins were performed as for the *E.coli* proteins, except that the NrdA (i.e. NrdA-a/NrdA-b) concentrations were 2.5–100 nM in the presence of effectors and/or substrates, while 25–500 nM NrdA was injected in experiments without nucleotides. The concentration ranges were chosen to cover 20–80% of saturated binding. The Aeh1 phage NrdA protein was injected for 6 min at 30 μl/min, and 20–51% of the theoretical maximum binding capacity was achieved. The non-specific binding to the reference cell was generally 2–4%. After each injection, the NrdA protein was allowed to dissociate in buffer for 10 min, followed by injection of 5–10 μl 10 mM glycine–HCl pH 2.0 and a further 3-min dissociation in running buffer. All experiments were performed at least twice. A prepared surface of Aeh1 phage NrdB was stable for approximately 3 days.

B. anthracis NrdE−NrdF interactions

The experiments were performed as above, with the NrdE concentration ranging between 10 nM to 2.5 μM in experiments with effectors and/or substrates, while 100 nM to 15 μM NrdE was injected in experiments without nucleotides. Both ranges gave 10–90% of saturated binding to the immobilized NrdF protein. Six to 14 different analyte concentrations were injected. The NrdE protein was injected for 2–8 min, and 35–65% of the theoretical maximum binding capacity was achieved. The non-specific binding to the

reference cell was generally 3–10%, but increased up to 20% for the highest NrdE analyte concentrations. Attempts to reduce the reference surface binding by increasing the salt and/or detergent (P20) concentrations generated unreliable data, and were not used further. Regeneration of the surface after injection involved 5 min dissociation in running buffer followed by 15 μl of 0.1 M HCl and 15 μl of 50 mM NaOH in 1 M NaCl, and finally 10–40 min of dissociation in the running buffer. A test of 14 injection cycles with 1 μM NrdE and the above regeneration procedure did not decrease the binding response despite 10% increase of the baseline level due to incomplete dissociation of bound NrdE. All experiments were performed three times, each time on a newly prepared SA sensor chip. A prepared surface of *B. anthracis* NrdF was stable for 2–3 days.

E.coli effector and substrate binding to immobilized NrdA protein

Effectors and substrates were injected in 10–13 different concentrations. Substrate and ATP analytes were injected in the range of 50 μM to 1.25 mM, substrate (in the presence of constant effector) from 10 to 750 μM, dTTP from 0.1 μM to 500 μM and dATP from 10 nM to 75 μM. The concentration ranges were chosen to cover 20–80% of saturated binding. The analytes were injected for 1–2 min, giving 19–52% of the theoretical maximum binding capacity, and a blank flow cell deactivated with biotin was used as reference cell. When the highest analyte concentrations were injected binding to the reference cell was typically 40–97% depending on the nucleotide combination. Dissociation in buffer 2–3 min was sufficient for regeneration of the binding surface. All experiments were repeated two to five times. NrdA protein exposed to the mild regeneration procedure described above was stable for 2–3 days.

Data analyses

SPR results were analyzed with the BIAevaluation 3.2 or 4.1 software (GE Healthcare). Reference cell binding and binding in the absence of analyte was subtracted from the data and the binding curve starting points were normalized prior to data fitting. The equilibrium dissociation constants K_{D1} and K_{D2} for dATP binding to the high (specificity) and low (overall activity) affinity binding sites in *E.coli* NrdA were calculated in KaleidaGraph using equation (1), where c is the analyte concentration, R_{M1} and R_{M2} are the maximum binding capacities for the two different binding sites and R is the instrument response:

$$R = \frac{c \times R_{M1}}{c \times K_{D1}} + \frac{c \times R_{M2}}{c \times K_{D2}} \tag{1}$$

Results

SPR immobilization of E.coli class Ia RNR via biotinylation

Previous RNR SPR studies have been performed using amino coupling of NrdB from mouse (Ingemarson and Thelander, 1996) or His-tagged NrdB from *E.coli* (Kasrayan *et al.*, 2004), but both studies reported difficulties in immobilizing the RNR proteins to the sensor chips. Also, there is no report of functional NrdA proteins being immobilized as

Table II. Effect of biotinylation on enzyme activity of *E.coli* NrdA and NrdB proteins

NrdA		NrdB	
Biotin/NrdA dimer	Enzyme activity[a] (%)	Biotin/NrdB dimer	Enzyme activity[a] (%)
0.5	76	0.7	73
1.1	71	0.9	58
2.4	56	1.7	60
4.4	47	2.5	56
6.6	13	6.9	14
8.5	4	7.8	3

[a]The activity of native NrdA and NrdB proteins were set as 100% activity (1560 and 3740 U/mg, respectively).

ligand on a sensor chip. We hypothesized that biotinylated proteins bound to SA sensor chips could be a better choice. To evaluate whether the streptavidin-biotin system could be used in RNR studies, we initially tested if the SPR buffer used or the biotin coupling affected the enzymatic activity. Table I shows that the activity of the three different class I RNR systems studied here was preserved in the 0.005% P20-containing buffer compared with the standard assay buffer. Using *E.coli* class Ia RNR, we titrated the NrdA and NrdB proteins with increasing molar excess of the biotin linker and assayed for enzymatic activity. At the optimal biotinylation level of one biotin molecule per NrdA or NrdB dimer the *E.coli* RNR enzymatic activity was approximately 70% for the NrdA protein and 60% for the NrdB protein compared with their unmodified counterparts (Table II). Increasing the ratio of biotin linker to protein resulted in lower activity of both the NrdA and the NrdB proteins. The biotinylated proteins were found to be capable of immobilization at several times higher densities to the SA sensor chips than the previous amino-coupled RNR proteins (data not shown), a crucial factor when monitoring binding of small molecules to immobilized proteins. Using the well-studied *E.coli* class Ia system allowed us to compare our data with past results generated by SPR and other methodologies. Notably, a previous SPR study (Kasrayan *et al.*, 2004) generated affinity constants for the NrdA–NrdB interactions that were two to seven times weaker than those obtained in solution from activity based K_D determinations (Climent *et al.*, 1991; Kasrayan *et al.*, 2004). Here we show that the low detergent concentration (0.005% P20) that is used throughout our study results in generally tighter interactions, with only a slight increase in non-specific binding to the reference cell. For instance, the non-specific binding increased from 2.1 to 2.6% (1 mM dATP in buffer A, 1 μM analyte *E.coli* NrdA and *E.coli* NrdB ligand).

Influence of substrate and effectors on E.coli NrdA–NrdB protein interactions

To gain further insight into allosteric regulation of RNRs, we undertook a comprehensive approach to study *E.coli* class Ia RNR subunit interactions using the biotin SPR methodology. As SPR biosensor studies are independent of enzyme activity measurements one can measure the isolated effects of substrates and effectors on holoenzyme interactions. We first examined the effects of dATP titration on subunit

Table III. *E.coli* NrdA–NrdB protein binding at different dATP concentrations

dATP (μM)	Biotin-coupled NrdB[a,b], K_D (μM)	Amino-coupled His$_6$-NrdB[a,b], K_D (μM)	Previous SPR analyses[a,b], K_D (μM)
1	0.16 ± 0.05	0.13 ± 0.1	1.8 ± 0.5
10	0.070 ± 0.005	0.057 ± 0.03	0.16 ± 0.02
100	0.035 ± 0.005	0.029 ± 0.005	0.11 ± 0.06
1000	0.029 ± 0.005	0.018 ± 0.000	0.023 ± 0.004

The K_D values were calculated using steady-state binding analysis.
[a]Amount of immobilized protein was 1200 or 3200 RU for the biotin-coupled NrdB (this study), 400–1200 RU for the amino-coupled NrdB (this study) and 1146 RU for the previous SPR analyses (Kasrayan *et al.*, 2004); the RU of the biosensor are directly proportional to mass and correspond to 1 pg/mm^2 of bound mass per RU (Jönsson *et al.*, 1991).
[b]Anumber of *E.coli* NrdA protein dimer bound per immobilized dimeric NrdB protein were 0.19–0.33 for the biotin-coupled NrdB (this study), 0.17–0.64 for the amino-coupled NrdB (this study) and 0.24–0.57 for the previous SPR analyses (Kasrayan *et al.*, 2004).

Table IV. Influence of allosteric effectors and substrates on *E.coli* NrdA–NrdB protein interactions

Effector	Substrate	K_D^a (μM)
None	None	3.81 ± 1.49
	1 mM CDP	2.67 ± 1.64
	1 mM GDP	3.34 ± 1.61
0.1 mM dTTP	None	1.59 ± 0.40
	1 mM CDP	1.34 ± 0.31
	1 mM GDP	1.07 ± 0.02
1 mM dTTP	None	0.63 ± 0.07
	1 mM CDP	0.95 ± 0.29
	1 mM GDP	0.98 ± 0.47

K_D values were calculated using steady-state binding analysis.
[a]Number of NrdA protein dimers bound per immobilized NrdB dimer were 0.24–0.43.

interactions and found that the NrdA–NrdB interaction was strengthened with increasing dATP concentrations, consistent with an inhibitory role of dATP binding to the allosteric regulatory site in the ATP cone. Stronger K_D values compared with the previous study, especially at the lower dATP concentrations, were obtained with the buffer A used here (Table III, Supplementary data, Fig. S1). The method of NrdB immobilization had almost no influence (Table III), suggesting that the biotin-linker molecules do not interfere with the subunit interactions.

We subsequently investigated NrdA–NrdB interactions under the influence of the substrates CDP or GDP, and the positive effector dTTP. In general, all interactions were considerably stronger as compared with the previous study (Table IV) (Kasrayan *et al.*, 2004). Interestingly, and in contrast to the previous study, there was no significant effect of substrate (CDP or GDP) on the NrdA–NrdB interaction. The allosteric effector dTTP induced a two to six times stronger interaction, with the stronger effect at the higher dTTP concentration (Table IV). Addition of substrate to the effector-containing binding experiments had no additional influence on the binding strength. We have previously reported an NrdA–NrdB subunit affinity of 0.95 ± 0.23 μM in the presence of 0.1 mM dTTP and CDP using the activity

assay-based affinity determination (Kasrayan *et al.*, 2004). The similar affinity constant of $1.34 \pm 0.31\ \mu M$ determined in the present SPR study (Table IV) indicates that affinity constants generated using our SPR method are comparable to those based on enzyme activity measurements.

Reichard and collaborators reported that ATP in combination with dTTP gave an inhibited RNR complex of large molecular weight (Brown and Reichard, 1969a,b). Recently, we confirmed that the ATP + dTTP effector combination induced formation of an octameric complex with 1:1 NrdA–NrdB composition even at low nucleotide concentrations (Rofougaran *et al.*, 2008). Here, we chose to study this unique aspect of the *E.coli* class Ia allosteric inhibition in more detail. Both dTTP and ATP alone strengthened the subunit interactions 6–8 times, but surprisingly 2 mM dTTP induced a 2.5-fold weaker complex compared with 1 mM dTTP (Tables IV and V). However, when ATP was titrated in the presence of 2 mM dTTP, the affinity increased up to 30 times at $100\ \mu M$ ATP (Table V) to a K_D almost as strong as that induced by 1 mM dATP (Table III). At higher ATP concentrations, the interaction is slightly weakened when ATP begins to compete with dTTP for binding to the specificity site. The obtained interaction strengths are in accordance with enzyme activity assays (Rofougaran *et al.*, 2008) where the maximum inhibition is seen around $200\ \mu M$ ATP + 2 mM dTTP, while the inhibition is partly relieved at 1 mM ATP + 2 mM dTTP (Rofougaran *et al.*, 2008).

Influence of substrate and effectors on Aeh1 phage (NrdA-a/NrdA-b)–NrdB protein interactions

To expand the knowledge of subunit interactions in allosteric regulation and to determine if the SPR procedure was generally applicable, we examined subunit interactions in two other RNR systems. First we investigated the influence of effectors and substrate on the atypical *A. hydrophila* phage Aeh1 class Ia RNR with a non-functional ATP cone and a split NrdA protein (Friedrich *et al.*, 2007). Despite the split NrdA protein, an active (NrdA-a/NrdA-b)$_2$NrdB$_2$ holoenzyme is formed (Friedrich *et al.*, 2007). The activity of the Aeh1 phage RNR was 71% in buffer A compared with the standard assay buffer (Table I). With 1.0 biotin-linker molecule per NrdB dimer, 55% of the activity was retained compared with non-biotinylated NrdB protein (data not shown). In the absence of effector and substrate, the Aeh1 NrdA-a/NrdA-b interaction with immobilized biotinylated NrdB (Table VI, Supplementary data, Fig. S2) was 20 times tighter than the corresponding interaction observed with the *E.coli* class Ia RNR (Table IV). Under the influence of effector dTTP, the affinity of the Aeh1 interaction increased four times, while dATP tightened the interaction an additional five times to the tightest RNR interaction we have observed so far ($K_D = 8$ nM). Inspection of the SPR sensorgrams revealed that effectors induced the formation of complexes with much slower dissociation rates as compared with experiments performed without effectors, or in the presence of substrate (Supplementary data, Fig. S2). In common with the *E.coli* RNR, substrate did not affect the affinity of the Aeh1 complex (Table VI). To validate the SPR data, we performed both an activity-based (Climent *et al.*, 1991) and a SPR-based K_D determination in the presence of 1 mM ATP and 0.7 mM substrate CDP. We obtained K_D $0.19 \pm 0.0029\ \mu M$ from the activity-based method in solution, and

Table V. *E.coli* NrdA–NrdB protein binding at different ATP concentrations in the presence of 2 mM dTTP

dTTP (mM)	ATP (μM)	K_D (μM)
None	100	2.87 ± 0.48
	2000	0.463 ± 0.009
2	None	1.56 ± 0.17
	1	0.76 ± 0.23
	10	0.17 ± 0.031
	100	0.054 ± 0.013
	200	0.057 ± 0.0057
	1000	0.098 ± 0.021
	2000	0.096 ± 0.014

The K_D values were calculated using steady-state binding analysis.

Table VI. Influence of allosteric effectors and substrates on Aeh1 phage (NrdA-a/Nrda-b)–NrdB protein interactions

Effector	Substrate	K_D^a (μM)
None	None	0.16 ± 0.048
	0.7 mM GDP	0.21 ± 0.06
1 mM dTTP	None	0.043 ± 0.001
	0.7 mM GDP	0.042 ± 0.003
None	0.7 mM CDP	0.25 ± 0.01
1 mM dATP	None	0.0084 ± 0.0025
	0.7 mM CDP	0.0133 ± 0.0047

The K_D values were calculated using steady-state binding analysis.
[a]Number of NrdA protein dimers bound per immobilized NrdB dimer were 0.20–0.51.

$0.25 \pm 0.051\ \mu M$ using the SPR method (data not shown). Thus, there is good correlation between the two methodologies.

Influence of substrate and effectors on B. anthracis NrdE–NrdF protein interactions

The third RNR system we analyzed was the class Ib RNR from *B. anthracis* that lacks an ATP cone, unlike the *E.coli* and phage Aeh1 enzymes (Torrents *et al.*, 2005). The strongly interacting *B. anthracis* NrdE–NrdF RNR has very low activity *in vitro* making it impossible to perform K_D determinations based on the activity measurements (Torrents and Sjöberg, unpublished). An activity-independent methodology such as SPR is thus required to examine subunit interactions. We found that the *B. anthracis* RNR was equally active in the SPR buffer (buffer A) as in the standard assay buffer (Table I), and retained 88% of the unmodified NrdF protein activity at 1.8 biotin linker molecules per NrdF dimer (data not shown). The biotinylated *B. anthracis* NrdF protein was immobilized to a high density on the SA sensor chips, and we measured the interaction with NrdE in the presence of 1 mM dTTP to be 35 nM (Table VII). This value is approximately the same as the corresponding Aeh1 phage subunit interactions, and 20 times stronger than the corresponding *E.coli* RNR interactions (Tables IV and VI). A notable difference was that high concentrations of dATP did not induce formation of a stronger complex of the *B. anthracis* components than did dTTP (Table VII, Supplementary data, Fig. S3). Similar to interactions of the *E.coli* and Aeh1 phage RNRs, substrate did not strengthen

the subunit interactions of *B. anthracis* NrdE-NrdF (Tables IV, VI and VII).

Binding of effectors and substrate to the E.coli NrdA protein

Biotinylated *E.coli* NrdA proteins with retained activity (Table II) could be efficiently immobilized onto SA biosensor chips. Previous attempts using amino coupling generated inactive immobilized NrdA protein (Kasrayan *et al*., 2004). To determine if NrdA functionality was preserved after

Table VII. Influence of allosteric effectors and substrates on *B. anthracis* NrdE–NrdF protein interactions

Effector	Substrate	K_D^a (μM)
None	None	0.51 ± 0.23
	1 mM CDP	0.46 ± 0.14
1 mM dTTP	None	0.035 ± 0.008
	1 mM CDP	0.041 ± 0.011
1 mM dATP	None	0.025 ± 0.006
	1 mM CDP	0.026 ± 0.006

K_D values were calculated using steady-state binding analysis.
[a]Number of NrdE protein dimers bound per immobilized NrdF dimer was 0.39–0.51.

Table VIII. K_D values for effectors or substrates bound to immobilized *E.coli* NrdA protein

Substrate or effector	Nucleotide addition	K_D (μM)	Previous K_D (μM)[a]
dTTP		2.8 ± 0.6	1.9
ATP		$153. \pm 38$ (both sites)	80
	1 mM dTTP	$221. \pm 0.0$ (activity site)	
dATP		0.15 ± 0.01 (specificity site)	0.43
		19.3 ± 3.9 (activity site)	6
	1 mM dTTP	8.3 ± 0.4 (activity site)	
CDP		$333. \pm 28$	
	0.1 mM dTTP	$136. \pm 3.6$	
GDP		$80. \pm 2.8$	
	0.1 mM dTTP	$22. \pm 2.8$	24[b]

K_D values obtained from steady-state analysis of binding.
[a]Data from Ormö and Sjöberg (1990).
[b]K_D value obtained at 40 μM dTTP (Ormö and Sjöberg, 1990).

immobilization on SA biosensor chips, and if the methodology could be used to screen small molecule binders to RNR, we examined nucleotide binding to NrdA. We obtained K_D values for the positive effectors dTTP and ATP (Table VIII) that were in accordance with the data obtained by ultrafiltration (Ormö and Sjöberg, 1990). It was not possible to resolve the two K_D values for ATP binding to the specificity and the overall activity sites, indicating that ATP has similar affinity for both sites (Fig. 1). A separate K_D for ATP binding to the overall activity site was instead obtained by occupying the specificity site with dTTP. The resultant binding constant of ATP for the activity site is close to that observed in the absence of dTTP (Table VIII), corroborating that the ATP-binding constants for the two different allosteric sites are similar when the NrdB protein is absent.

In contrast, the affinities of dATP for the specificity site and the overall activity site differed by more than one order of magnitude and the separate K_D values were readily calculated using equation (1) (Fig. 1B). Blocking the specificity site with dTTP gave a lower K_D for dATP binding to the overall activity site than in the absence of dTTP (Table VIII). This indicates cross-talk between the specificity and activity sites as has been observed in the past (Brown *et al*., 1967; Brown and Reichard, 1969a,b; Larsson Birgander *et al*., 2004).

One important observation was that K_D values for nucleotides with weak binding could be determined. This is exemplified in Table VIII for CDP. Whereas the K_D of 80 μM for GDP has been observed before (Ormö and Sjöberg, 1990), the K_D of approximately 300 μM for CDP has not previously been observed. Binding of the substrates in the presence of dTTP revealed that substrate binding increased 2.5–3.6 times (CDP and GDP respectively) in the presence of the effector nucleotide. Thus, we believe this methodology is suitable for investigating binding of other small molecules to RNR such as potential inhibitors.

Discussion

The activity of RNRs is controlled by sophisticated allosteric regulation that relies on the differential affinity of nucleotides for two regulatory sites, the specificity site and the overall
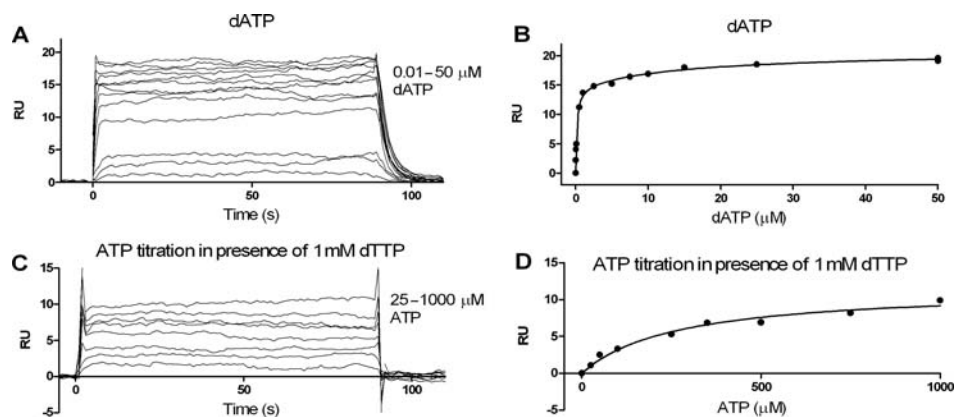
Fig. 1. SPR results of the allosteric effectors dATP and ATP bound to immobilized *E.coli* NrdA protein. (**A**) SPR curves at dATP concentrations of 10 nM to 50 μM (reference cell binding and binding in absence of analyte subtracted). (**B**) Mean dATP responses plotted against concentration of dATP and fitted to the two-K_D model (1) described in the section Materials and Methods. (**C**) SPR curves at ATP concentrations of 25–1000 μM in the presence of 1 mM dTTP. (**D**) Mean ATP response plotted against concentration of ATP and fitted to steady-state kinetics.

activity site. Binding of nucleotides to the two regulatory sites modulates overall RNR activity in response to cellular concentrations of ATP and dATP, and also balances the production of dNDPs from NDPs by influencing what nucleotide is bound in the active site. Accurately determining the relative affinities of nucleotides for each of these sites and their effect on holoenzyme interactions are therefore crucial to understanding the biological role that nucleotides play in fine-tuning RNR activity. In the current study we have presented a SPR method based on biotinylation to investigate interactions between subunits of RNRs in response to nucleotides and to study binding of nucleotides to RNRs. The biotin immobilization methodology allows maximal exposure of any interaction surface of the immobilized protein as biotinylation is introduced randomly at primary amines and conveys a 30.5-Å spacer between the target protein and the biotin. Further advantages are that the method seems generally applicable to RNRs as all tested RNR proteins could be immobilized by the strong biotin−streptavidin interaction, and that biotinylated proteins can be assayed for preserved enzyme activity prior to immobilization. Investigating RNR class I subunit and nucleotide interactions are challenging tasks due to the complex nature of the RNR systems. SPR analyses can potentially produce association and dissociation rate constants, but the complexity necessitated the use of steady-state calculations for the K_D determinations throughout this study. Firstly, the catalytic components NrdA and NrdE are homodimers in equilibrium with monomers, especially at low protein concentrations (Larsson Birgander *et al.*, 2004; Rofougaran *et al.*, 2008). Secondly, the $\alpha_2\beta_2$ *E.coli* complex forms via two consecutive steps, an initial bimolecular contact between one polypeptide each in α_2 and β_2 with a K_D of 13 μM, followed by a 17-fold favored unimolecular rearrangement to the pairwise polypeptide interactions of the holoenzyme (Climent *et al.*, 1992). Thirdly, allosterically inhibiting nucleotide combinations favor $\alpha_4\beta_4$ forms of the *E.coli* NrdAB complex (Brown and Reichard, 1969a,b; Rofougaran *et al.*, 2008). As the sensor chip dextran matrix is flexible enough to support dimerization of human growth hormone receptors (Cunningham and Wells, 1993) it is likely that the matrix also supports the equilibrium transitions in the RNR systems (as discussed below). Despite the complicating equilibria we were able to achieve affinity data comparable with data derived from other methods when available (Climent *et al.*, 1991; Kasrayan *et al.*, 2004).

We studied the subunit interactions of the *E.coli* and Aeh1 phage class Ia RNRs and the *B. anthracis* class Ib RNRs and, when available, found good correlation with the corresponding activity assay-based affinity data in solution (Climent *et al.*, 1991; Kasrayan *et al.*, 2004; Rofougaran *et al.*, 2008). This set of RNRs was chosen to represent a diversity of ATP cones and allosteric regulation among class I RNRs. In all three systems, we showed that interactions between the RNR subunits were strengthened in the presence of effector nucleotides, with subunit interactions increasing between 4 and 15 times in the presence of dTTP. Each enzyme had a different response to dATP, confirming the importance of the ATP-cone domain in response to dATP-mediated regulation. The *E.coli* class Ia holoenzyme with a functional ATP cone was strengthened 22 times in the presence of dATP compared with dTTP (Tables III and IV), while the interaction of the *B. anthracis* holoenzyme that

lacks the ATP-cone domain was not significantly different in response to dATP or dTTP (Table VII). Of particular interest was our finding that the interaction of the Aeh1 phage class Ia RNR with a non-functional ATP cone was tightened only five times by dATP compared with dTTP (Table VI). Furthermore, the Aeh1 phage RNR forms an $\alpha_4\beta_4$ complex in the presence of 50 μM dATP (Crona *et al.*, to be published), although much less efficient than the *E.coli* class Ia RNR (Brown and Reichard, 1969a,b; Rofougaran *et al.*, 2008). Thus, although the Aeh1 phage class Ia RNR has a non-functional ATP cone and lacks dATP-inhibition, it has remnant features of the dATP response.

In addition, the comparative studies demonstrated the wide range of subunit interaction strengths seen in different RNR systems. The *B. anthracis* and Aeh1 phage RNRs are active at interaction strengths where the *E.coli* class Ia enzyme is inhibited. The Aeh1 phage interaction strengths are the tightest reported, and may be an adaptation of the fragmented NrdA-a/NrdA-b large subunit to promote interactions with NrdB to form an active complex. We believe this result shows that the relative interaction strengths within each RNR system under different conditions are more important than absolute affinities. For the *E.coli* class Ia enzyme the inhibitory combination of ATP + dTTP induced a complex almost as tight as the dATP-inhibited complex. The tight *E.coli* NrdAB complexes formed in the presence of either dATP or ATP + dTTP already at low nucleotide concentrations (50 μM) are known to be $\alpha_4\beta_4$ oligomers (Rofougaran *et al.*, 2008). Thus, our strong K_D values indicate formation of $\alpha_4\beta_4$ complexes on the sensor chips, in accordance with the previous data on dimerization between individually immobilized molecules on sensor chips (Cunningham and Wells, 1993).

In contrast to the prominent strengthening of the RNR subunit interactions by the allosteric effector nucleotides, presence of substrate nucleotides did not affect the subunit interactions in any of the three studied RNR systems in our SPR studies. This result is in contrast to the substrate effects observed in a previous SPR study where measured dissociation constants were not physiological, likely due to high detergent (Kasrayan *et al.*, 2004). Previous GEMMA experiments show that the *E.coli* NrdAB interactions are not influenced by 50 μM substrate (Rofougaran *et al.*, 2008). However, we have observed (Hofer, Crona and Sjöberg, unpublished) that holoenzyme complex formation was promoted by substrate in the *E.coli* NrdA mutant N238A with impaired NrdA dimerization (Larsson Birgander *et al.*, 2005) and also to a minor extent in the *B. anthracis* class Ia RNR where the NrdE subunit is mainly monomeric even in the presence of 50 μM dATP (Torrents *et al.*, to be published). Thus, even though subunit interactions are mainly strengthened by binding of allosteric effectors, we cannot exclude that substrate under certain circumstances influence subunit interactions, possibly by stabilizing weak α-dimers.

Recently, Hassan *et al.* (2008) utilized fluorophore-labeled His-tagged *E.coli* NrdB to report a 10 times stronger NrdAB affinity compared with the affinities reported here. However, the fluorophore-labeled NrdB activity was one to three orders of magnitude lower than the wild-type activity, and a 50-fold excess of NrdA was used (Hassan *et al.*, 2008). We suggest that the SPR method presented in our study is a more versatile method than the fluorophore method that requires the introduction of three site-specific mutations in *E.coli* NrdB

for fluorophore coupling, whereas any wild-type RNR component can be biotinylated, checked for preserved enzyme activity and immobilized on the SA biosensor chip.

One important application of the biotinylation methodology reported here is the first successful immobilization of a functional *E.coli* NrdA protein on SPR sensor chips. We evaluated the method's potential by performing a comprehensive investigation of nucleotide binding to the NrdA protein. Our results correlated well with earlier equilibrium dialysis and ultrafiltration studies (Brown and Reichard, 1969a,b; Ormö and Sjöberg, 1990), and extended the range of analyses to nucleotides with comparatively weak binding that has not been accessible with earlier used methods (e.g. substrate CDP with K_D of 0.3 ± 0.03 mM).

In summary, the SPR methodology presented here is suitable both for studying RNR protein–protein interactions and protein–small molecule interactions on immobilized RNRs using biotinylation as the only pre-requirement. In addition, the methodology is fast and could in principle be used for high throughput screening of chemical compounds that bind RNRs for use as antibacterial, antiviral or anticancer agents. One attractive feature of the method is the ability to simultaneously screen binding of compounds to different RNR proteins from several species on the same sensor chip to identify compounds that selectively interact with pathogen rather than host RNRs.

References

Aravind,L., Wolf,Y.I. and Koonin,E.V. (2000) *J. Mol. Microbiol. Biotechnol.*, **2**, 191–194.

Atkin,C.L., Thelander,L., Reichard,P. and Lang,G. (1973) *J. Biol. Chem.*, **248**, 7464–7472.

Brown,N.C. and Reichard,P. (1969a) *J. Mol. Biol.*, **46**, 25–38.

Brown,N.C. and Reichard,P. (1969b) *J. Mol. Biol.*, **46**, 39–55.

Brown,N.C., Larsson,A. and Reichard,P. (1967) *J. Biol. Chem.*, **242**, 4272–4273.

Climent,I., Sjöberg,B.-M. and Huang,C.Y. (1991) *Biochemistry*, **30**, 5164–5171.

Climent,I., Sjöberg,B.-M. and Huang,C.Y. (1992) *Biochemistry*, **31**, 4801–4807.

Cunningham,B.C. and Wells,J.A. (1993) *J. Mol. Biol.*, **234**, 554–563.

Eriksson,M., Uhlin,U., Ramaswamy,S., Ekberg,M., Regnström,K., Sjöberg,B.-M. and Eklund,H. (1997) *Structure*, **5**, 1077–1092.

Friedrich,N.C., Torrents,E., Gibb,E.A., Sahlin,M., Sjöberg,B.-M. and Edgell,D.R. (2007) *Proc. Natl Acad. Sci. USA*, **104**, 6176–6181.

Hassan,A.Q., Wang,Y., Plate,L. and Stubbe,J. (2008) *Biochemistry*, **47**, 13046–13055.

Ingemarson,R. and Thelander,L. (1996) *Biochemistry*, **35**, 8603–8609.

Jönsson,U., Fagerstam,L., Ivarsson,B., Johnsson,B., Karlsson,R., Lundh,K., Löfås,S., Persson,B., Roos,H. and Rönnberg,I., *et al.* (1991) *Biotechniques*, **11**, 620–627.

Kasrayan,A., Birgander,P.L., Pappalardo,L., Regnström,K., Westman,M., Slaby,A., Gordon,E. and Sjöberg,B.-M. (2004) *J. Biol. Chem.*, **279**, 31050–31057.

Larsson Birgander,P., Kasrayan,A. and Sjöberg,B.-M. (2004) *J. Biol. Chem.*, **279**, 14496–14501.

Larsson Birgander,P., Bug,S., Kasrayan,A., Dahlroth,S.L., Westman,M., Gordon,E. and Sjöberg,B.-M. (2005) *J. Biol. Chem.*, **280**, 14997–15003.

Mathews,C.K. (2006) *FASEB J.*, **20**, 1300–1314.

Mock,M. and Fouet,A. (2001) *Annu. Rev. Microbiol.*, **55**, 647–671.

Nordlund,P. and Reichard,P. (2006) *Annu. Rev. Biochem.*, **75**, 681–706.

Nordlund,P., Sjöberg,B.-M. and Eklund,H. (1990) *Nature*, **345**, 593–598.

Ormö,M. and Sjöberg,B.-M. (1990) *Anal. Biochem.*, **189**, 138–141.

Rofougaran,R., Vodnala,M. and Hofer,A. (2006) *J. Biol. Chem.*, **281**, 27705–27711.

Rofougaran,R., Crona,M., Vodnala,M., Sjöberg,B.-M. and Hofer,A. (2008) *J. Biol. Chem.*, **283**, 35310–35318.

Sambrook,J., Fritsch,E.F. and Maniatis,T. (1989) *Molecular Cloning: A Laboratory Manual*. 2nd edn, Cold Spring Harbor Laboratory Press.

Sjöberg,B.M., Hahne,S., Karlsson,M., Jörnvall,H., Göransson,M. and Uhlin,B.E. (1986) *J. Biol. Chem.*, **261**, 5658–5662.

Thelander,L., Sjöberg,B.-M. and Eriksson,S. (1978) *Methods Enzymol.*, **51**, 227–237.

Torrents,E., Sahlin,M., Biglino,D., Gräslund,A. and Sjöberg,B.-M. (2005) *Proc. Natl Acad. Sci. USA*, **102**, 17946–17951.

Torrents,E., Sahlin,M. and Sjöberg,B.-M. (2008) The ribonucleotide reductase family—genetics and genomics. In Andersson,K.K. and Uversky,V.N. (eds), *Molecular Anatomy and Physiology of Proteins: Ribonucleotide Reductase*. Nova Science Publishers, pp. 17–77.

Uhlin,U. and Eklund,H. (1994) *Nature*, **370**, 533–539.

von Döbeln,U. and Reichard,P. (1976) *J. Biol. Chem.*, **251**, 3616–3622.